

Global Biogeochemical Cycles

RESEARCH ARTICLE

10.1029/2019GB006300

Key Points:

- Average global monthly PIC standing stock integrated over the top 100 m is estimated to be 27.04 Tg
- Average global PIC turnover rate is estimated to be on the order of 7 days
- The Great Calcite Belt region strongly influences the seasonal and interannual variability of the global PIC standing stock

Correspondence to:

W. M. Balch,
bbalch@bigelow.org

Citation:

Hopkins, J., Henson, S. A., Poulton, A. J., & Balch, W. M. (2019). Regional characteristics of the temporal variability in the global particulate inorganic carbon inventory. *Global Biogeochemical Cycles*, 33. <https://doi.org/10.1029/2019GB006300>

Received 31 MAY 2019

Accepted 30 SEP 2019

Accepted article online 22 OCT 2019

Regional Characteristics of the Temporal Variability in the Global Particulate Inorganic Carbon Inventory

Jason Hopkins^{1,2} , Stephanie A. Henson³ , Alex J. Poulton^{3,4} , and William M. Balch¹ 

¹Bigelow Laboratory for Ocean Sciences, East Boothbay, ME, USA, ²Now at the Ordnance Survey, Southampton, UK,

³Ocean Biogeochemistry and Ecosystems, National Oceanography Centre Southampton, European Way, Southampton, UK, ⁴Now at the Lyell Centre for Earth and Marine Sciences and Technology, Heriot-Watt University, Edinburgh, UK

Abstract Coccolithophores are a biogeochemically important calcifying group of phytoplankton that exert significant influence on the global carbon cycle. They can modulate the air-sea flux of CO₂ through the processes of photosynthesis and calcification and, as one of the primary contributors to the oceanic particulate inorganic carbon (PIC) pool, promote the export of organic carbon to depth. Here we present the first interannually resolved, global analysis of PIC standing stock. Average, global PIC standing stock in the top 100 m is estimated to be 27.04 ± 4.33 Tg PIC, with turnover times of ~7 days, which suggests PIC is likely removed by active processes such as grazing or rapid sinking, mediated through biogenic packaging (i.e., fecal pellets). We find that the Southern Hemisphere plays a significant role in the variability in PIC inventories and that interannual variability in PIC standing stock is driven primarily by variability in the midlatitude oceanic gyres and regions within the Great Calcite Belt of the Southern Ocean. Our results provide a framework against which future changes in global PIC standing stocks may be assessed.

1. Introduction

1.1. Coccolithophores and the Carbon Cycle

Coccolithophores are calcifying phytoplankton that influence the global carbon cycle through the production of particulate inorganic carbon (PIC), which can modify both the air-sea flux of CO₂ and the export of carbon to depth (Rost & Riebesell, 2004). These single-celled haptophyte algae produce an external covering (coccospHERE) of interlocking calcium carbonate scales (coccoliths) and have been significant contributors to the carbonate cycle since the Jurassic period (Hay, 2004). As autotrophs, coccolithophores contribute to the biological carbon pump and the uptake of CO₂ through the photosynthetic production of organic carbon. The calcification process, however, results in the production of CO₂, which can act in opposition to carbon sequestration by the biological carbon pump (Rost & Riebesell, 2004). Previous work (Harlay et al., 2010; Robertson et al., 1994; Shutler et al., 2013) has suggested that calcification during blooms of the coccolithophore *Emiliania huxleyi* might alter the air-sea flux of CO₂, although to date, the impact of this has only been explored on a limited regional basis (Balch et al., 2016; Bates, 2007).

Any change in CO₂ uptake caused by calcification may be offset to some extent by enhanced transport of particulate organic carbon to depth. The transfer of detached coccoliths alone to the deep sea environment is an inefficient process given that their micron diameter size is likely to result in a relatively slow settling velocity (~11–14 cm/day; Balch, Kilpatrick, & Trees, 1996; Honjo, 1976). In the deeper ocean, where the water column may be undersaturated with respect to calcium carbonate (Holligan & Robertson, 1996), such a slow rate of descent through the water column would increase exposure time, the efficiency of dissolution, and effectively shorten the remineralization length scale. In addition, evidence from sediment traps suggests that coccoliths and coccospHERes are more likely to be transported to depth when incorporated within fecal pellets or marine snow (Steinmetz, 1994). The relationship between the flux of sinking organic matter and mineral fluxes, in particular, fluxes of calcium carbonate (Klaas & Archer, 2002), suggests that the aggregation of PIC with organic particles may be beneficial for the efficient export of carbon (Armstrong et al., 2002). Such ballasting could increase sinking speeds and hence the export efficiency of both the inorganic and organic carbon (Bach et al., 2016). If mineral ballasting does indeed enhance the flux of organic carbon (Bach et al., 2016; Klaas & Archer, 2002; Sanders et al., 2010), areas of high PIC standing stock may represent regions of increased carbon sequestration to the deep sea or possibly to the sediments.

Calcifying organisms, such as coccolithophores, are thought to be at risk from decreasing oceanic pH, known as ocean acidification (Bach et al., 2015; Doney et al., 2009). The impact of climate change on these key biogeochemically relevant organisms, however, is not straight forward, with apparently contradictory laboratory responses to decreasing pH (Iglesias-Rodriguez et al., 2008; Riebesell et al., 2000) and time series observations that suggest both decreased calcification (Freeman & Lovenduski, 2015) and increased coccolithophore abundance (Rivero-Calle et al., 2015) over recent decades, despite decreasing ocean pH.

Given the biogeochemical significance of coccolithophores and the potential for them to act as sentinels for the effects of climate change, accurate estimates of PIC standing stocks and assessments of associated interannual variability are needed to provide a benchmark for longer-term studies. In addition, a contemporary estimate of PIC inventory is fundamental for our understanding of PIC turnover in the global ocean and its implications for the carbon cycle.

1.2. Satellite Detection of Coccolithophores

Satellite observations of coccolithophore blooms date back to the advent of ocean color remote sensing (Holligan et al., 1983; Le Fevre et al., 1983). In Case I waters, where the optical properties are driven primarily by those of water and phytoplankton rather than nonphytoplanktonic sources (Mobley, 1994), blooms of coccolithophores (e.g., *E. huxleyi*) can result in patches of high reflectivity, and associated unique optical characteristics (Balch, Kilpatrick, Holligan, et al., 1996) that can be used to estimate PIC concentration. Ocean color satellite-acquired PIC concentration is currently derived from a merged two-band (Balch et al., 2005) or three-band (Gordon et al., 2001) algorithm. A previous estimate of global PIC standing stock used radiometric data for 2002 from the Moderate Resolution Imaging Spectroradiometer (MODIS) sensor on board the National Aeronautics and Space Administration's TERRA satellite (Balch et al., 2005). Seasonally averaged PIC concentration data were integrated uniformly over euphotic zone depth and 10° latitudinal bands to establish a global PIC standing stock estimate of 18.8 ± 2.56 Tg PIC (Balch et al., 2005). These data showed that the majority of the PIC standing stock was associated with the Westerlies and Trades biomes (Longhurst, 1998) and that coastal provinces made comparatively lower contributions to the global PIC inventory compared to open ocean regions (Balch et al., 2005). The study also identified an area in the Southern Ocean that made a relatively large contribution to the global PIC inventory between October and March, geographically located north of the Polar Front and south of the Subtropical Front, with highest PIC concentrations over the Patagonian Shelf, decreasing to the east from the Atlantic, Indian, Australian, and Pacific sectors of the Southern Ocean. This region, now referred to as the Great Calcite Belt (GCB), was later shown to be associated with elevated concentrations of coccolithophores and detached coccoliths (Balch et al., 2011, 2014).

Here, we revisit the first global PIC estimates of Balch et al. (2005) and take advantage of a multiyear (2003–2014) AQUA MODIS data set of satellite-derived PIC concentration and an empirically derived relationship between surface and depth-integrated water column PIC concentration (Balch et al., 2018). We use this to generate a contemporary estimate for depth-integrated global PIC standing stock and, for the first time, multiyear estimates of the spatial and temporal variability in the global oceanic PIC inventory.

2. Materials and Methods

2.1. Satellite Detection of PIC

Global, Level 3, mapped, monthly AQUA MODIS 9 km PIC data (R2014.0 reprocessing) for the years 2003 to 2014 were downloaded from the National Aeronautics and Space Administration Ocean Color data repository (<http://oceandata.sci.gsfc.nasa.gov/>). In order to maximize computational efficiency, these data sets were resized to one degree by 1° spatial resolution using nearest neighbor interpolation. The method currently used to estimate PIC concentration from remotely sensed measurements uses a combined two-band or three-band algorithm (Balch et al., 2005; Gordon et al., 2001). The PIC algorithm is generally considered to be a Case I algorithm (Balch et al., 2005; Morel & Prieur, 1977). The optical properties of Case I waters are correlated with phytoplankton and their associated by-products, whereas in Case II waters, retrievals can be influenced by other constituents, such as suspended sediments. We have therefore chosen to exclude satellite derived data obtained from water column depths of less than 200 m and focus our interpretation of the output from our model to the open ocean (i.e., Case I waters only). The error of the

monthly binned, 1° spatially binned, surface PIC estimates was $\pm 0.024\text{-}\mu\text{g}$ PIC per liter (i.e., $\pm 0.002\text{ mmol/m}^3$; see Table 2 in Balch et al., 2005).

2.2. Vertical Structure in Coccolithophore PIC Standing Stock

In order to derive an estimate of PIC standing stock, the masked 1° by 1° pixel average PIC concentration (moles C/m³) was integrated over depth. When contemplating the appropriate depth parameter to integrate over, consideration must be given to whether light availability (i.e., euphotic depth) or mixing (i.e., mixed layer depth) has the biggest influence on the distribution of coccolithophores and the production and distribution of coccoliths through the water column. Previous work (Balch et al., 2005) integrated PIC concentration uniformly over the euphotic zone depth (in the absence of vertical information on the PIC distributions). Here, however, we made use of a new empirical relationship (equation (1)) derived from a global data set of field observations, collected over 17 cruises and every major ocean basin, of in situ water column and surface PIC concentrations (Balch et al., 2018). This global relationship integrates surface satellite PIC concentration to 100-m depth and reflects the influence of both biological and physical processes (e.g., reduced photosynthesis and light reduction with depth) and, as such, is likely to be more accurate than simple integration assuming uniform profiles:

$$\text{PIC}_{100\text{m}} [\text{mmol C/m}^2] = 40.555 * \text{PIC}_{\text{surface}} [\text{mmol C/m}^3]^{0.560} \quad (1)$$

The root-mean-square error of this equation is ± 0.233 log units (Balch et al., 2018; see their Table 2).

Depth-integrated PIC concentration was then converted from molar units to a mass standing stock (g C/m²). Total global standing stock (in units of teragrams of carbon) was determined by multiplying standing stock by the latitudinally varying area of each 1° by 1° pixel.

2.3. Longhurst Biogeochemical Provinces

In order to assess regional variability in global PIC inventory, standing stock data were subdivided into Longhurst provinces using a shape file (www.marineregions.org/downloads.php). Longhurst (1998) provinces divide the global ocean initially into four biomes (Polar, Westerlies, Trades, and Coastal) that differ in terms of water column stability, nutrient availability, and light levels. These biomes are further separated into 54 provinces based on biological and oceanographic parameters such as chlorophyll distribution, mixed layer depth, and euphotic zone depth (Longhurst, 1998). Given our decision to exclude data from water depths <200 m, averaged data for provinces that occur close to the coast will contain only data from depths in excess of the bathymetric mask.

2.4. Assessing Seasonal Variability and Ranking of Provincial Influences

Seasonal variability was assessed using the coefficient of variation (standard deviation divided by the mean of the 12 years of monthly data) in PIC standing stock for each province. In addition, monthly climatologies of PIC standing stock were determined from the arithmetic mean of 12 years (2003–2014) of monthly standing stock data. Global interannual variability in PIC standing stock was determined by subtracting the global climatological mean seasonal cycle from the corresponding time series of monthly mean global PIC standing stock data for 2003 to 2014. Interannual variability for each province was similarly calculated and compared to this global estimate of interannual variability using the Pearson product-moment correlation coefficient. This enabled an objective ranking of the degree to which each province influences global PIC standing stock interannual variability, with provinces that have a higher correlation coefficient being deemed more influential to overall global interannual variability than provinces with lower coefficients.

3. Results

3.1. Spatial-Temporal Variability of Integrated PIC

Spatial and temporal variability in monthly climatologies of integrated PIC standing stock are shown in Figure 1. Standing stocks of PIC in the Southern Hemisphere begin to increase in October with evidence of relatively high ($>0.2\text{ g C/m}^2$) inventories developing predominantly off the coasts of Chile and Namibia. The spatial extent of these areas evolves through November, with relatively high PIC standing stocks extending out across the southern subtropical Pacific and Atlantic. The beginnings of a band of relatively high PIC inventory can be observed straddling the region where the South Atlantic, Indian, and South

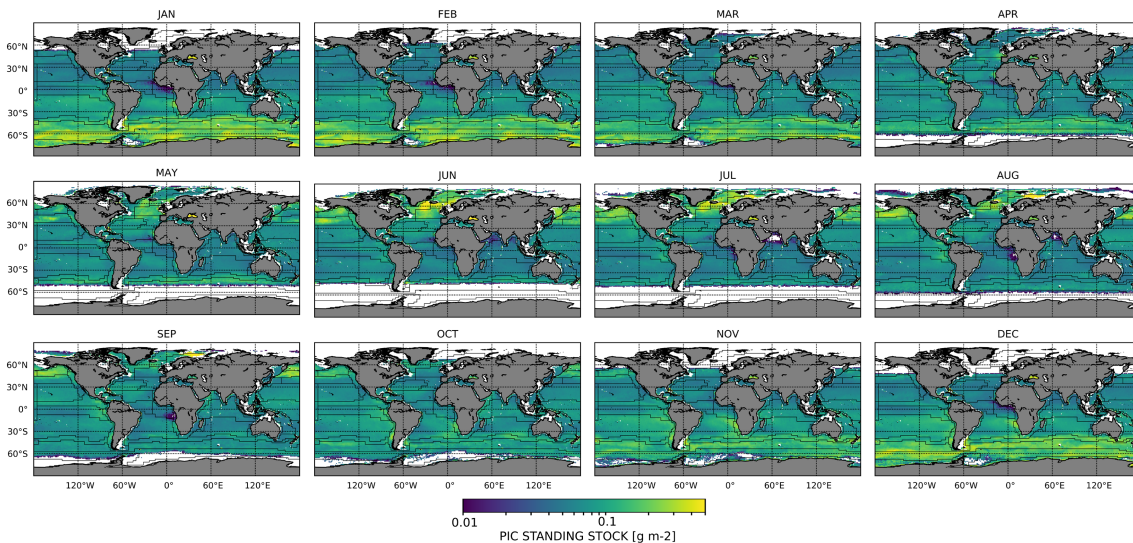


Figure 1. Average, monthly global PIC standing stocks derived from AQUA Moderate Resolution Imaging Spectroradiometer PIC concentration data (2003–2014) integrated to 100 m (g/m^2). Black lines indicate Longhurst provinces (Longhurst, 1998). White areas represent regions of no data due to low winter Sun angle, water depth <200 m, persistent cloud or ice cover. PIC = particulate inorganic carbon.

Pacific Oceans meets the Southern Ocean. The magnitude and extent of this band develops further in December and advances poleward into the Southern Ocean.

The relatively high PIC standing stocks observed initially off the coasts of Chile and Namibia begin to decline in January; however, the band that encircles the globe below $\sim 40^\circ\text{S}$ (the GCB) persists into February and to a lesser extent in March. There is evidence of relatively high PIC standing stocks ($> \sim 0.2 \text{ g/m}^2$) beginning to develop in the high-latitude North Atlantic in May, which reach their greatest extent and magnitude ($> \sim 0.4 \text{ g C/m}^2$) by June. It is also at this time that PIC standing stocks begin to develop in the North Pacific. While PIC inventories start to decline in the North Atlantic in July and August, they continue to develop in the North Pacific through August and persist until September.

The average monthly global PIC standing stock for years 2003 to 2014 is estimated to be $27.04 \pm 4.33 \text{ Tg C}$ (± 1 standard deviation; Table 1). Highest average, monthly global PIC inventory is observed in January (34.05 Tg C) with the lowest recorded in June (22.01 Tg C), both extremes are within two standard deviations of the mean (hence, the monthly variability is not significantly different from the mean at a 95% confidence level). A time series of 100-m-integrated global PIC shows annual cycles of PIC, with highest values observed near the beginning of the austral summer and minima near the beginning of the austral winter (Figure 2). We explore the influence that each Longhurst province has on seasonal variability by correlating the time series data from each province with the global, mean time series of data (Figure 3). This highlights a hemispherical imbalance in PIC standing stock, which is evident when the global total PIC inventory is viewed over time (Figure 2). The lesser influence of standing stocks in the Northern Hemisphere during the boreal summer (June to August) compared to those observed during the austral summer (December to February), relative to the total global PIC standing stock, is clear.

Table 1

Average, Monthly, Total Global PIC Standing Stock in Tg PIC

JAN	FEB	MAR	APR	MAY	JUN	JUL	AUG	SEP	OCT	NOV	DEC
34.05	31.89	28.97	24.82	22.47	22.01	22.09	23.75	24.70	26.40	30.12	33.27

Note. The 100 m-integrated PIC standing stock values have a root-mean-square error of ± 0.233 log units (Balch et al., 2018). PIC = particulate inorganic carbon.

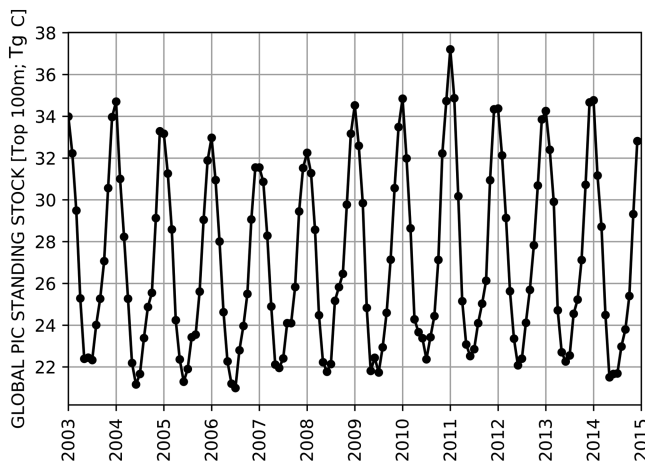


Figure 2. Globally integrated, monthly PIC standing stock time series (in teragrams of PIC). PIC = particulate inorganic carbon.

3.2. Regional Contributions to the Global PIC Signal and Temporal Anomalies

The difference in contributions to global PIC standing stock is further emphasized in Figure 3. Here we compare PIC standing stock time series data from each province to the global total PIC standing stock time series using correlation coefficients. The Southern Hemisphere regions are generally positively correlated with the total global PIC standing stock, while those in the Northern Hemisphere tend to be negatively correlated. These high-correlation coefficients are likely driven by the strong seasonal cycle in global and regional PIC concentrations. In terms of temporal variability in the PIC inventory time series data between 2003 and 2014, our results show that the highest coefficient of variation (standard deviation/mean) is observed predominantly in provinces in the high latitudes with those in the mid- and lower latitudes appearing to have relatively weak seasonal variability (Figure 4). Some of the lowest coefficients of variation are observed in the oceanic gyre provinces (e.g., Provinces 7, 22, 23, 35, 37, and 38). Our results suggest that there is little seasonal variability in PIC standing stocks here.

We use 12 years of monthly PIC standing stock anomalies to assess the influence that each province has on interannual variability in global PIC standing stock (Figure 5). These anomaly data suggest that global PIC standing stocks were generally lower than the mean global climatology prior to 2008, increased relative to the climatology between 2008 and 2014, and show evidence of a decline again after 2014. We further assess the contribution that interannual variability in PIC standing stock from each province makes relative to the global time series of 100-m-integrated PIC standing stock (Figure 6). Globally, the Southern Ocean appears to be highly influential in regard to global PIC standing stock interannual variability. In terms of key regions, PIC standing stock anomalies from the Indian Southern Subtropical Gyre (23), North Pacific Equatorial Counterurrent (39), West Pacific Warm Pool, South Pacific Subtropical Gyre (37), Sub-Antarctic (52), and Antarctic (53) provinces have the highest correlations with global PIC standing stock anomalies. Provinces from the northern hemisphere are less correlated with global PIC standing stock anomalies than provinces

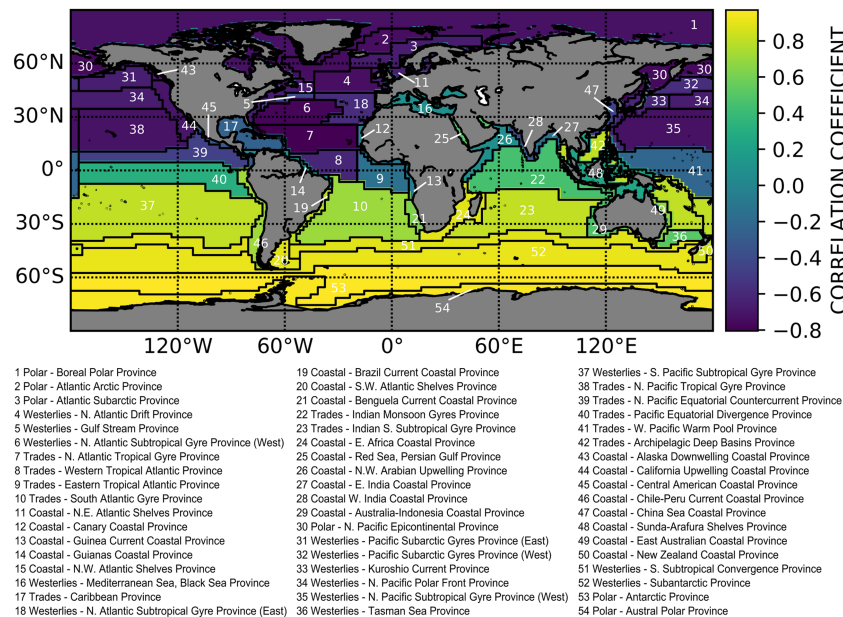


Figure 3. Correlation of province PIC standing stock time series with global PIC standing stock time series (Figure 2). Green to yellow represents a positive correlation coefficient, while green to blue indicates a negative correlation coefficient. Provinces with no color are where correlation is not significant at the 5% level. PIC = particulate inorganic carbon.

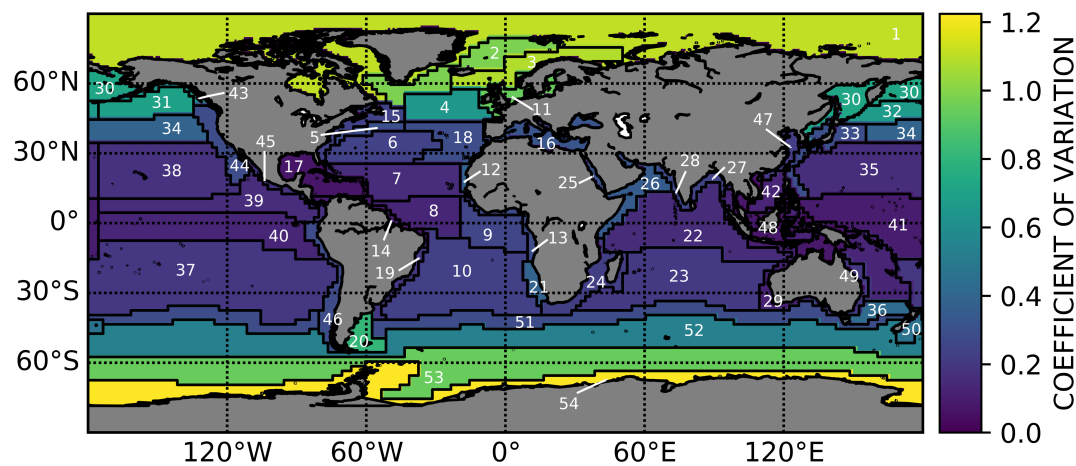


Figure 4. Temporal variability in Longhurst (1998) province particulate inorganic carbon standing stock as measured by the coefficient of variability (standard deviation/mean). Yellow indicates high variability within the seasonal time series, while blue indicates low variability. Numbers refer to the Longhurst (1998) provinces. See Figure 3 for key to province numbers.

from the Southern Hemisphere, suggesting that the northern hemisphere has a lesser influence on global interannual variability in PIC inventory than the Southern Hemisphere.

4. Discussion

4.1. Extending Surface PIC Concentrations to Depth and the Global Inventory

Early work developing phytoplankton biomass estimates from satellite-derived data-integrated surface estimates of chlorophyll to 1-m depth, as no reliable method existed at that time to extend those data further down the water column (Yoder et al., 1993). Our global analysis of PIC standing stock variability utilizes a unique relationship, developed from an extensive database of in situ measurements, to extend surface satellite PIC concentration data to 100-m depth. Techniques such as integrating satellite chlorophyll data over the mixed layer depth (e.g., Brown et al., 1995) or PIC data over the euphotic zone depth (e.g., Balch et al., 2005) was previously employed to extend surface estimates to depth. However, in the absence of information on the vertical distribution pattern of PIC, previous work involved the assumption that surface concentration was uniformly distributed over depth. The empirical relationship used here provides a more robust representation of the global surface to depth relationship of PIC concentration and follows similar work that used relationships developed from depth profiles of chlorophyll concentration to integrate surface values to depth (Balch et al., 1992; Behrenfeld et al., 2006; Morel, 1988; Platt et al., 1988; Platt & Herman, 1983). The decision to use the surface-depth relationship developed by Balch et al. (2018) over other depth integrals (e.g., mixed layer depth or euphotic depth) represents an advance on previous work that assumed homogenous PIC distribution with depth. The choice of 100-m integration depth is justified in Balch et al. (2018) as being the depth that produces the coefficients that closest match those of the euphotic zone integrations of in situ data for global data sets.

Our estimate of global, monthly average PIC standing stock of 27.04 ± 4.33 Tg C is ~40% higher than the previous estimate of global PIC standing stock derived from satellite data (Balch et al., 2005), which may be due to methodological differences. The previous assessment used radiance data derived from TERRA MODIS with the two-band PIC algorithm used to determine PIC concentration. In addition, the data were binned seasonally over 10° bands and integrated uniformly over the depth of the euphotic zone. Our estimate used monthly AQUA MODIS PIC concentration

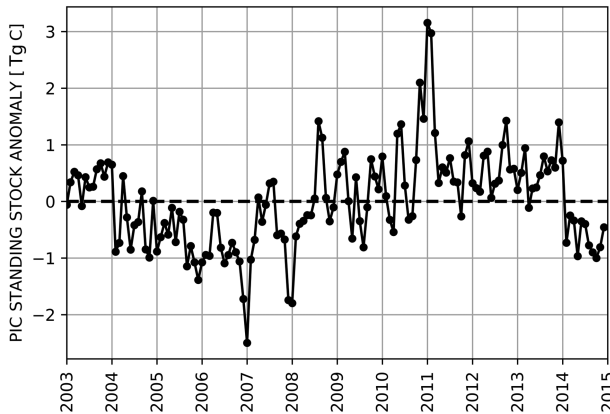


Figure 5. Interannual variability in average monthly global PIC standing stock integrated over the top 100 m of the water column (Tg PIC). Data represent anomalies from the annual climatology of PIC standing stock. PIC = particulate inorganic carbon.

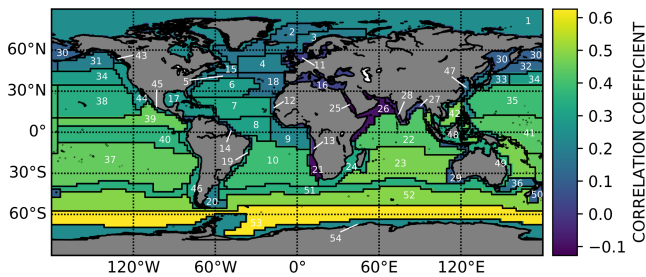


Figure 6. Correlation of province PIC 100-m-integrated standing stock anomalies with global PIC standing stock anomalies (Figure 5). Yellow represents relatively high correlation coefficient and blue a relatively low correlation coefficient. Provinces with no color are where correlation is not significant at the 5% level. See Figure 3 for key to province numbers. PIC = particulate inorganic carbon.

data derived from the merged PIC algorithm (R2014.0 reprocessing), integrated over 1° spatial bins, and to 100-m depth using the above-noted empirical surface to depth relationship. We believe our estimate to be more representative as it is based on four factors: (a) a longer time series of data; (b) higher spatial resolution averaging; (c) the merged two- and three-band algorithm, the coefficients of which have been refined over the years through increased shipboard validation; and (d) the above empirically derived relationship for integrating surface PIC concentrations to depth. However, it should be noted that monthly composite satellite data are derived from the average of a variable number of observations per month, dependent upon the number of overpasses, amount of cloud cover, and Sun angle. Therefore, in some areas, these monthly averages will have been derived from variable numbers of observations (e.g., some regions will have lower numbers of binned observations in the monthly mean than others).

4.2. Turnover of PIC in the Upper 100 m of the Sea

Recently, Hopkins and Balch (2018) produced new integrated global calcification rate estimates using an algorithm based on coccolithophore ecophysiology principals, rather than empirically derived relationships based on shipboard measurements (e.g., Balch et al., 2007). Our recently published global calcification rate estimate was 1.43 Pg PIC/year (Hopkins & Balch, 2018). Dividing the above-discussed average global PIC standing stock (27.04 Tg) by the average global calcification rate, and assuming quasi steady state, gives an average turnover time of 6.95 days, which is almost identical to an earlier estimate of 6.86 days (Balch et al., 2005). Turnover times for PIC calculated from in situ data range from 3–7 days (Poulton et al., 2006, 2013). Estimates from seven major field campaigns ranged from ~7–50 days (Balch et al., 2007). Long turnover times of PIC, on the order of tens of days, would be suggestive of low ballasted, slow-sinking particles. On the other hand, rapid turnover rates of PIC, at time scales of days (as indicated here by these remotely sensed data) would suggest active, rather than passive, removal processes (Poulton et al., 2007), for example, grazing by zooplankton (Mayers et al., 2018) or aggregation into large, well-ballasted, fast sinking particles. This observation also agrees with other work (Honjo et al., 2008) that suggests that the dominant removal process for PIC in the global ocean may not simply be independent sinking or in situ dissolution of coccoliths.

We can also generate a visual representation of the spatial variability of PIC turnover times in each Longhurst province (Figure 7). Our analysis shows that across the majority of the global ocean, turnover times are relatively rapid (~5 days); however, across the Indian Ocean and extending out from the central West Pacific, turnover times can slow to longer than 15 days (similar to the longer turnover times observed by Balch et al., 2007). Long turnover rates observed in the high latitudes may also be due to poorer statistics for calcification rate determinations (and indeed, standing stock determinations) due to fewer reliable satellite retrievals in regions with persistent cloud cover and low Sun angles.

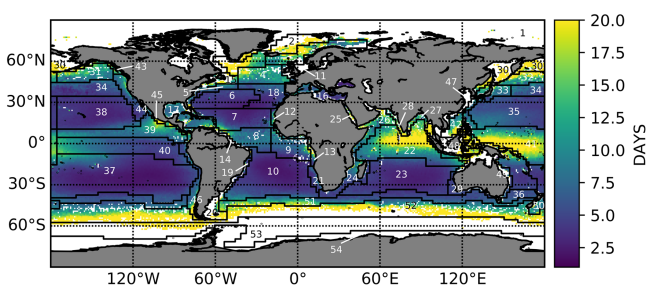


Figure 7. Spatial variability in PIC standing stock turnover times, calculated by dividing the integrated PIC standing stock by the integrated calcite production rate estimated according to Hopkins and Balch (2018). See Figure 3 for key to Longhurst (1998) province numbers. White areas represent regions where turnover times are >20 days or areas of no data due to low winter sun angle, water depth < 200 m, persistent cloud or ice cover. PIC = particulate inorganic carbon.

Just how well, though, do these turnover times, derived from space-based measurements, compare with measured PIC residence times? Using ^{14}C -derived calcification rate measurements and PIC standing stock measurements taken along an equatorial transect at 140°W , Balch and Kilpatrick (1996) estimated PIC residence times to be 3–15 days. Our average estimates of turnover times from the Longhurst provinces closest to the area sampled (39: N. Pacific Equatorial Countercurrent; 40: Pacific Equatorial Divergence) are 9.3 and 7.1 days, respectively. In the Atlantic Ocean, PIC residence times are estimated to be on the order of 3 days (range < 1 to 6.8 days) from 40°S to $\sim 50^{\circ}\text{N}$ (Poulton et al., 2006). Our turnover estimates from the provinces that cover the cruise track for these data (18: N. Atlantic Subtropical Gyre [East]; 7: N. Atlantic Subtropical Gyre; 8: Western Tropical Atlantic; 10: South Atlantic Gyre) are 4–8 days. It

should be noted that our estimates are derived from annual averages and thus may miss the short temporal scale and small spatial scale variability expected in the natural environment. However, our estimates are within the ranges measured in situ. The median turnover time from the data in Figure 7 is 6.6 days in line with the estimates of Balch et al. (2005) and that estimated using alternative calcification rate data (Balch et al., 2005).

4.3. PIC Disparities Between Hemispheres

Our monthly estimates of global spatial (Figure 1) and temporal (Figure 2) variability in PIC standing stocks highlight a disparity between hemispheres. There is evidence of higher PIC standing stocks associated with regions mainly within the Southern Hemisphere (Figure 2), which are likely the result of there being a larger open ocean area there. The band of relatively high PIC standing stock that encircles the Southern Ocean, north of the Polar Front and south of the Subtropical Front, from November to March (Figure 1) corresponds with the location of the GCB (Balch et al., 2011, 2014). The influence of this region on global PIC standing stock estimates is emphasized when PIC standing stocks are considered in terms of Longhurst provinces. Within the GCB, regions such as the Southern Subtropical Convergence (51) and Sub-Antarctic (52) are associated with relatively high average PIC standing stocks during the austral spring and summer (Figure 1) that are comparable in magnitude to regions from the high-latitude Northern Hemisphere such as the Atlantic Arctic (2), the Atlantic Subarctic (3), and North Atlantic Drift (4) provinces, regions that are often synonymous with large-scale blooms of coccolithophores (Brown & Yoder, 1994; Holligan et al., 1993; Shutler et al., 2013). In addition, time series of PIC standing stock data from provinces within the GCB are strongly correlated with the total, global PIC standing stock time series (Figure 3), suggesting that this region is highly influential on the global ocean seasonal standing stock variability.

4.4. Potential Influence of Case II Coastal Waters on PIC Concentrations

We have chosen to exclude immediate coastal waters from this analysis using a 200 m bathymetric mask, which means that the global estimates presented here are likely to be conservative. In addition, there is evidence of relatively high PIC concentrations in the area immediately adjacent to Antarctica, especially over the Antarctic shelf, which should also be treated with caution. These waters would include the Austral Polar province (54) and to some extent, the Antarctic province (53). It has been reported that *E. huxleyi* abundance is typically low in the high latitude Southern Ocean (Charalampopoulou et al., 2016; Holligan et al., 2010) and other phenomena such as highly reflective glacial flour or reflective loose ice could produce sufficient reflectance to adversely overestimate satellite PIC retrievals in this specific region (Balch, 2018; Balch et al., 2011; Trull et al., 2018). High-latitude *Phaeocystis* blooms might also abnormally elevate the reflectance (Alvain et al., 2008). Note, though, that the provenance of the highly reflecting material in these waters near the coast of Antarctica is still not known and these areas should not be considered part of the GCB.

It is somewhat difficult to assess the impact that excluding Case II waters has on our estimate. On the one hand coccolithophore blooms have been widely reported in coastal regions (e.g., Balch et al., 1991; Poulton et al., 2013); however, the impact that resuspended material may have on satellite-derived PIC estimates is difficult to quantify (Mitchell et al., 2016). By choosing to exclude Case II waters, we believe our estimate to be a conservative one and highlights the need for further research into satellite derived observations in coastal regions (e.g., see Kopelevich et al., 2014, for an example of a coastal coccolithophore algorithm that takes into account both the abundance of coccolithophores and the influence of local river input of suspended material).

4.5. Major Regional Influences on the Global PIC

The predominant regions that appear to influence global interannual variability in PIC standing stocks are largely ocean gyre regions such as the South Atlantic Gyre (10), the North Pacific Tropical Gyre (38), and the North (35) and South (37) Pacific Subtropical Gyre provinces. These typically low productivity regions tend to have relatively low surface PIC concentrations but subsurface PIC maxima in the upper 100 m (Balch et al., 2018). Thus, subsurface maxima combined with the sheer size of these provinces could be major factors influencing interannual variability in the global PIC inventory. The actual driver (or drivers) of interannual variability, though, remain unclear as attempts to correlate global and individual province anomaly data with indices of climate-scale variability, such as the Multivariate El Niño–Southern Oscillation Index,

North Atlantic Oscillation, Southern Ocean Index and Pacific Decadal Oscillation, were inconclusive (data not shown).

Our results suggest that provinces from the Polar and Westerlies biomes are associated with some of the highest PIC standing stocks (Figure 1). We also find that provinces from the Westerlies and Trade biomes exhibit the highest correlation with global PIC standing stock anomalies (cf. Balch et al., 2005). Provinces from the GCB appear to be driving much of the interannual variability observed in global PIC inventories (Figure 6). In terms of identifying the source of such high PIC standing stock estimates, the area associated with the Southwest Atlantic Shelves province (20) has previously been shown to be associated with some of the highest coccolithophore concentrations found in the Southern Ocean (Balch et al., 2014; Smith et al., 2017). Observations of coccolithophore populations across the Pacific sector of the Southern Ocean (Saavedra-Pellitero et al., 2014) suggest that coccolithophores are responsible for the elevated PIC standing stocks and associated interannual variability observed across provinces that make up the GCB.

4.6. Concluding Remarks

This study has used a novel relationship between surface and depth-integrated PIC concentration to extend surface measurements to 100-m depth and, as such, provides a contemporary estimate of integrated PIC standing stock in the global ocean. The Southern Hemisphere appears to play a significant role in the temporal and spatial variability in PIC standing stock, with a large number of Southern Ocean provinces exhibiting a strong positive correlation with global PIC standing stock over interannual time scales. Our results suggest that this relatively large area of ocean may have a greater influence on PIC standing stocks than the northern hemisphere. In particular we note the influence of the GCB, which appears to have a significant influence on global PIC standing stock variability. Observations suggest that PIC concentrations may be declining in this area (Freeman & Lovenduski, 2015), and our results suggest that any such changes, particularly within regions of the Southern Hemisphere (e.g., GCB), could have global implications for PIC standing stocks and thus potentially, the carbon cycle. While our work has not been conducted on the time scales required to identify trends caused by climate change (e.g., ~40 years; Henson et al., 2010), it serves as a baseline against which future shifts in PIC standing stock can be assessed.

Acknowledgments

The authors wish to thank the NASA Ocean Biology Processing Group at the Goddard Space Flight Center (Maryland, USA) for the production and access to the ocean color data used in this analysis (<http://oceancolor.gsfc.nasa.gov>). We would also like to thank Bruce Bowler, Dave Drapeau, Laura Lubelczyk, Emily Lyczkowski, and Catherine Mitchell for their efforts in the collection of in situ data that were used to generate the surface-to-water column PIC relationship. Satellite data used in this paper are available online (<https://oceancolor.gsfc.nasa.gov>). In situ calcification rate data are available from <https://seabass.gsfc.nasa.gov> website. They can also be found at PANGEA (<https://www.pangaea.de/>) under <https://doi.org/10.1594/PANGAEA.888182> (Daniels et al., 2018; Poultney et al., 2018). J. H. and W. M. B. were supported by NASA Grants NNX14AL92G, NNX14AQ43A, NNX14AQ41G, and 80NSSC19K0043 to W. M. B.

References

- Alvain, S., Moulin, C., Dandonneau, Y., & Loisel, H. (2008). Seasonal distribution and succession of dominant phytoplankton groups in the global ocean: A satellite view. *Global Biogeochemical Cycles*, 22, GB3001. <https://doi.org/10.1029/2007GB003154>
- Armstrong, R. A., Lee, C., Hedges, J. I., Honjo, S., & Wakeham, S. G. (2002). A new, mechanistic model for organic carbon fluxes in the ocean based on the quantitative association of POC with ballast minerals. *Deep Sea Research Part II: Topical Studies in Oceanography*, 49, 219–236.
- Bach, L. T., Boxhammer, T., Larsen, A., Hildebrandt, N., Schulz, K. G., & Riebesell, U. (2016). Influence of plankton community structure on the sinking velocity of marine aggregates. *Global Biogeochemical Cycles*, 30, 1145–1165. <https://doi.org/10.1002/2016GB005372>
- Bach, L. T., Riebesell, U., Gutowska, M. A., Federwisch, L., & Schulz, K. G. (2015). A unifying concept of coccolithophore sensitivity to changing carbonate chemistry embedded in an ecological framework. *Progress in Oceanography*, 135, 125–138. <https://doi.org/10.1016/j.pocean.2015.04.012>
- Balch, W. M. (2018). The ecology, biogeochemistry, and optical properties of coccolithophores. *Annual Review of Marine Science*, 10(1), 71–98. <https://doi.org/10.1146/annurev-marine-121916-063319>
- Balch, W. M., Bates, N. R., Lam, P. J., Twining, B. S., Rosengard, S. Z., Bowler, B. C., et al. (2016). Factors regulating the Great Calcite Belt in the Southern Ocean and its biogeochemical significance. *Global Biogeochemical Cycles*, 30, 1124–1144. <https://doi.org/10.1002/2016GB005414>
- Balch, W. M., Bowler, B. C., Drapeau, D. T., Lubelczyk, L. C., & Lyczkowski, E. (2018). Vertical distributions of coccolithophores, PIC, POC, biogenic silica, and chlorophyll a throughout the global ocean. *Global Biogeochemical Cycles*, 32, 2–17. <https://doi.org/10.1002/2016GB005614>
- Balch, W. M., Drapeau, D. T., Bowler, B. C., & Booth, E. (2007). Prediction of pelagic calcification rates using satellite measurements. *Deep-Sea Research Part II-Topical Studies in Oceanography*, 54(5–7), 478–495. <https://doi.org/10.1016/j.dsrr.2006.12.006>
- Balch, W. M., Drapeau, D. T., Bowler, B. C., Lyczkowski, E. R., Lubelczyk, L. C., Painter, S. C., & Poultney, A. J. (2014). Surface biological, chemical, and optical properties of the Patagonian Shelf coccolithophore bloom, the brightest waters of the Great Calcite Belt. *Limnology and Oceanography*, 59(5), 1715–1732. <https://doi.org/10.4319/lo.2014.59.5.1715>
- Balch, W. M., Drapeau, D. T., Bowler, B. C., Lyczkowski, E., Booth, E. S., & Alley, D. (2011). The contribution of coccolithophores to the optical and inorganic carbon budget during the Southern Ocean Gas Exchange Experiment: New evidence in support of the “Great Calcite Belt” hypothesis. *Journal of Geophysical Research*, 116, C00F06. <https://doi.org/10.1029/2011JC006941>
- Balch, W. M., Evans, R., Brown, J., Feldman, G., McClain, C., & Esaias, W. (1992). The remote sensing of ocean primary productivity: Use of a new data compilation to test satellite algorithms and waters. *Journal of Geophysical Research*, 97(91), 2279–2293. <https://doi.org/10.1029/1999JC000043>
- Balch, W. M., Gordon, H. R., Bowler, B. C., Drapeau, D. T., & Booth, E. S. (2005). Calcium carbonate measurements in the surface global ocean based on Moderate-Resolution Imaging Spectroradiometer data. *Journal of Geophysical Research*, 110, C07001. <https://doi.org/10.1029/2004JC002560>

- Balch, W. M., Holligan, P. M., Ackleson, S. G., & Voss, K. J. (1991). Biological and optical properties of mesoscale coccolithophore blooms in the Gulf of Maine. *Limnology and Oceanography*, 36(4), 629–643.
- Balch, W. M., & Kilpatrick, K. (1996). Calcification rates in the equatorial Pacific along 140 degrees W. *Deep-Sea Research Part II*, 43(4–6), 971–993. [https://doi.org/10.1016/0967-0645\(96\)00032-X](https://doi.org/10.1016/0967-0645(96)00032-X)
- Balch, W. M., Kilpatrick, K. A., Holligan, P. M., Harbour, D. S., & Fernandez, E. (1996). The 1991 coccolithophore bloom in the central North Atlantic. 2. Relating optics to coccolith concentration. *Limnology and Oceanography*, 41(8), 1684–1696. <https://doi.org/10.4319/lo.1996.41.8.1684>
- Balch, W. M., Kilpatrick, K. A., & Trees, C. C. (1996). The 1991 coccolithophore bloom in the central North Atlantic. 1. Optical properties and factors affecting their distribution. *Limnology and Oceanography*, 41(8), 1669–1683. <https://doi.org/10.4319/lo.1996.41.8.1669>
- Bates, N. R. (2007). Interannual variability of the oceanic CO₂ sink in the subtropical gyre of the North Atlantic Ocean over the last two decades. *Journal of Geophysical Research*, 112, C09013. <https://doi.org/10.1029/2006JC003759>
- Behrenfeld, M. J., O'Malley, R. T., Siegel, D. A., McClain, C. R., Sarmiento, J. L., Feldman, G. C., et al. (2006). Climate-driven trends in contemporary ocean productivity. *Nature*, 444(7120), 752–755. <https://doi.org/10.1038/nature05317>
- Brown, C. W., Esaias, W. E., & Thompson, A. M. (1995). Predicting phytoplankton composition from space—Using the ratio of euphotic depth to mixed-layer depth: An evaluation. *Remote Sensing of Environment*, 53(3), 172–176. [https://doi.org/10.1016/0034-4257\(95\)00099-M](https://doi.org/10.1016/0034-4257(95)00099-M)
- Brown, C. W., & Yoder, J. A. (1994). Coccolithophorid blooms in the global ocean. *Journal of Geophysical Research*, 99(C4), 7467–7482. <https://doi.org/10.1029/93JC02156>
- Charalampopoulou, A., Poulton, A. J., Bakker, D. C. E., Lucas, M. I., Stinchcombe, M. C., & Tyrrell, T. (2016). Environmental drivers of coccolithophore abundance and calcification across Drake Passage (Southern Ocean). *Biogeosciences*, 13(21), 5917–5935. <https://doi.org/10.5194/bg-13-5917-2016>
- Daniels, C. J., Poulton, A. J., Balch, W. M., Marañón, E., Adey, T., Bowler, B. C., et al. (2018). A global compilation of coccolithophore calcification rates. *Earth System Science Data*, 10(4), 1859–1876. <https://doi.org/10.5194/essd-10-1859-2018>
- Doney, S. C., Fabry, V. J., Feely, R. A., & Kleypas, J. (2009). Ocean acidification: The other CO₂ Problem. *Annual Review of Marine Science*, 1(1), 169–192. <https://doi.org/10.1146/annurev.marine.010908.163834>
- Freeman, N. M., & Lovenduski, N. S. (2015). Decreased calcification in the Southern Ocean over the satellite record. *Geophysical Research Letters*, 42, 1834–1840. <https://doi.org/10.1002/2014GL062769>
- Gordon, H. R., Boynton, G. C., Balch, W. M., Groom, S. B., Harbour, D. S., & Smyth, T. J. (2001). Retrieval of coccolithophore calcite concentration from SeaWiFS imagery. *Geophysical Research Letters*, 28(8), 1587–1590. <https://doi.org/10.1029/2000GL012025>
- Harlay, J., Borges, A. V., van der Zee, C., Delille, B., Godoi, R. H. M., Schiettecatte, L. S., et al. (2010). Biogeochemical study of a coccolithophore bloom in the northern Bay of Biscay (NE Atlantic Ocean) in June 2004. *Progress in Oceanography*, 86(3–4), 317–336. <https://doi.org/10.1016/j.pocean.2010.04.029>
- Hay, W. W. (2004). Carbonate fluxes and calcareous nannoplankton. In H.-R. Thiersten, & J. R. Young (Eds.), *Coccolithophores: from molecular processes to global impact*, (pp. 509–528). Heidelberg: Springer-Verlag.
- Henson, S. A., Sarmiento, J. L., Dunne, J. P., Bopp, L., Lima, I., Doney, S. C., et al. (2010). Detection of anthropogenic climate change in satellite records of ocean chlorophyll and productivity. *Biogeosciences*, 7(2), 621–640. <https://doi.org/10.5194/bg-7-621-2010>
- Holligan, P. M., Charalampopoulou, A., & Hutson, R. (2010). Seasonal distributions of the coccolithophore, *Emiliania huxleyi*, and of particulate inorganic carbon in surface waters of the Scotia Sea. *Journal of Marine Systems*, 82(4), 195–205. <https://doi.org/10.1016/j.jmarsys.2010.05.007>
- Holligan, P. M., Fernández, E., Aiken, J., Balch, W. M., Boyd, P., Burkill, P. H., et al. (1993). A biogeochemical study of the coccolithophore, *Emiliania huxleyi*, in the North Atlantic. *Global Biogeochemical Cycles*, 7(4), 879–900. <https://doi.org/10.1029/93GB01731>
- Holligan, P. M., & Robertson, J. E. (1996). Significance of ocean carbonate budgets for the global carbon cycle. *Global Change Biology*, 2(2), 85–95. <https://doi.org/10.1111/j.1365-2486.1996.tb00053.x>
- Holligan, P. M., Viollier, M., Harbour, D. S., Camus, P., & Champagne-Phillipe, M. (1983). Satellite and ship studies of coccolithophore production along a continental shelf edge. *Nature*, 304(5924), 339–342. <https://doi.org/10.1038/304339a0>
- Honjo, S. (1976). Coccoliths: Production, transportation and sedimentation. *Marine Micropaleontology*, 1, 65–79. [https://doi.org/10.1016/0377-8398\(76\)90005-0](https://doi.org/10.1016/0377-8398(76)90005-0)
- Honjo, S., Manganini, S. J., Krishfield, R. A., & Francois, R. (2008). Particulate organic carbon fluxes to the ocean interior and factors controlling the biological pump: A synthesis of global sediment trap programs since 1983. *Progress in Oceanography*, 76(3), 217–285. <https://doi.org/10.1016/j.pocean.2007.11.003>
- Hopkins, J., & Balch, W. M. (2018). A new approach to estimating coccolithophore calcification rates from space. *Journal of Geophysical Research: Biogeosciences*, 123, 1447–1459. <https://doi.org/10.1002/2017JG004235>
- Iglesias-Rodriguez, M. D., Halloran, P. R., Rickaby, R. E. M., Hall, I. R., Colmenero-Hidalgo, E., Gittins, J. R., et al. (2008). Phytoplankton calcification in a high-CO₂ world. *Science*, 320(5874), 336–340. <https://doi.org/10.1126/science.1154122>
- Klaas, C., & Archer, D. E. (2002). Association of sinking organic matter with various types of mineral ballast in the deep sea: Implications for the rain ratio. *Global Biogeochemical Cycles*, 16(4), 1116. <https://doi.org/10.1029/2001GB001765>
- Kopelevich, O., Burenkov, V., Sheberstov, S., Vazyulya, S., Kravchishina, M., Pautova, L., et al. (2014). Satellite monitoring of coccolithophore blooms in the Black Sea from ocean color data. *Remote Sensing of Environment*, 146, 113–123. <https://doi.org/10.1016/j.rse.2013.09.009>
- Le Feuvre, J., Viollier, M., Le Corre, P., Dupouy, C., & Grall, J.-R. (1983). Remote sensing observations of biological material by LANDSAT along a tidal thermal front and their relevancy to the available field data. *Estuarine, Coastal and Shelf Science*, 16(1), 37–50. [https://doi.org/10.1016/0272-7714\(83\)90093-8](https://doi.org/10.1016/0272-7714(83)90093-8)
- Longhurst, A. R. (1998). *Ecological geography of the sea*. San Diego: Academic Press.
- Mayers, K. M. J., Poulton, A. J., Daniels, C. J., Wells, S. R., Woodward, E. M. S., Tarrant, G. A., et al. (2018). Growth and mortality of coccolithophores during spring in a temperate Shelf Sea (Celtic Sea, April 2015). *Progress in Oceanography*, 177, 1–13. <https://doi.org/10.1016/j.pocean.2018.02.024>
- Mitchell, C., Cunningham, A., & McKee, D. (2016). Derivation of the specific optical properties of suspended mineral particles and their contribution to the attenuation of solar irradiance in offshore waters by ocean color remote sensing. *Journal of Geophysical Research: Oceans*, 121, 104–117. <https://doi.org/10.1002/2015JC011056>
- Mobley, C. D. (1994). Optical properties of water. In *Light and Water: radiative transfer in natural waters* (pp. 60–144).
- Morel, A. (1988). Optical modelling of the upper ocean in relation to its biogenous matter content (Case I waters). *Journal of Geophysical Research*, 93, 749–768.

- Morel, A., & Prieur, L. (1977). Analysis of variations in ocean color. *Limnology and Oceanography*, 22(4), 709–722. <https://doi.org/10.4319/lo.1977.22.4.0709>
- Platt, T., & Herman, A. W. (1983). Remote sensing of phytoplankton in the sea: Surface-layer chlorophyll as an estimate of water-column chlorophyll and primary production. *International Journal of Remote Sensing*, 4(2), 343–351. <https://doi.org/10.1080/01431168308948552>
- Platt, T., Sathyendranath, S., Caverhill, C. M., & Lewis, M. R. (1988). Ocean primary production and available light: Further algorithms for remote sensing. *Deep Sea Research Part A, Oceanographic Research Papers*, 35(6), 855–879. [https://doi.org/10.1016/0198-0149\(88\)90064-7](https://doi.org/10.1016/0198-0149(88)90064-7)
- Poulton, A. J., Adey, T. R., Balch, W. M., & Holligan, P. M. (2007). Relating coccolithophore calcification rates to phytoplankton community dynamics: regional differences and implications for carbon export. *Deep Sea Research Part II: Topical Studies in Oceanography*, 54(5-7), 538–557. <https://doi.org/10.1016/j.dsrr.2006.12.003>
- Poulton, A. J., Daniels, C. J., Balch, W. M., Marañón, E., Adey, T., Bowler, B. C., et al. (2018). Global compilation of coccolithophore calcification measurements from unperturbed water samples. PANGAEA. <https://doi.org/10.1594/PANGAEA.888182>
- Poulton, A. J., Painter, S. C., Young, J. R., Bates, N. R., Bowler, B., Drapeau, D., et al. (2013). The 2008 *Emiliania huxleyi* bloom along the Patagonian Shelf: Ecology, biogeochemistry, and cellular calcification. *Global Biogeochemical Cycles*, 27, 1023–1033. <https://doi.org/10.1002/2013GB004641>
- Poulton, A. J., Sanders, R., Holligan, P. M., Stinchcombe, M. C., Adey, T. R., Brown, L., & Chamberlain, K. (2006). Phytoplankton mineralization in the tropical and subtropical Atlantic Ocean. *Global Biogeochemical Cycles*, 20, GB4002. <https://doi.org/10.1029/2006GB002712>
- Riebesell, U., Zondervan, I., Rost, B., Tortell, P. D., Zeebe, R. E., & Morel, F. M. M. (2000). Reduced calcification of marine plankton in response to increased atmospheric CO₂. *Nature*, 407(6802), 364–367. <https://doi.org/10.1038/35030078>
- Rivero-Calle, S., Gnanadesikan, A., Del Castillo, C. E., Balch, W., & Guikema, S. D. (2015). Multidecadal increase in North Atlantic coccolithophores and the potential role of rising CO₂. *Science*, 346(November), 1–8. <https://doi.org/10.1126/science.aaa8026>
- Robertson, J. E., Robinson, C., Turner, D. R., Holligan, P., Watson, A. J., Boyd, P., et al. (1994). The impact of a coccolithophore bloom on oceanic carbon uptake in the northeast Atlantic during summer 1991. *Deep Sea Research Part I: Oceanographic Research Papers*, 41(2), 297–314. [https://doi.org/10.1016/0967-0637\(94\)90005-1](https://doi.org/10.1016/0967-0637(94)90005-1)
- Rost, B., & Riebesell, U. (2004). Coccolithophores and the biological pump: responses to environmental change. In H.-R. Thiersten, & J. R. Young (Eds.), *Coccolithophores: from molecular processes to global impact*, (pp. 99–126). Heidelberg: Springer-Verlag.
- Saavedra-Pellitero, M., Baumann, K.-H., Flores, J.-A., & Gersonde, R. (2014). Biogeographic distribution of living coccolithophores in the Pacific sector of the Southern Ocean. *Marine Micropaleontology*, 109, 1–20. <https://doi.org/10.1016/j.marmicro.2014.03.003>
- Sanders, R., Morris, P. J., Poulton, A. J., Stinchcombe, M. C., Charalampopoulou, A., Lucas, M. I., & Thomalla, S. J. (2010). Does a ballast effect occur in the surface ocean? *Geophysical Research Letters*, 37, L08602. <https://doi.org/10.1029/2010GL042574>
- Shutler, J. D., Land, P. E., Brown, C. W., Findlay, H. S., Donlon, C. J., Medland, M., et al. (2013). Coccolithophore surface distributions in the North Atlantic and their modulation of the air-sea flux of CO₂ from 10 years of satellite Earth observation data. *Biogeosciences*, 10(4), 2699–2709. <https://doi.org/10.5194/bg-10-2699-2013>
- Smith, H. E. K., Poulton, A. J., Garley, R., Hopkins, J., Lubelczyk, L. C., Drapeau, D. T., et al. (2017). The influence of environmental variability on the biogeography of coccolithophores and diatoms in the Great Calcite Belt. *Biogeosciences*, 14(21), 4905–4925. <https://doi.org/10.5194/bg-14-4905-2017>
- Steinmetz, J. C. (1994). Sedimentation of coccolithophores. In A. Winter, & W. G. Siesser (Eds.), *Coccolithophores*, (pp. 179–198). Cambridge: Cambridge University Press.
- Trull, T. W., Passmore, A., Davies, D. M., Smit, T., Berry, K., & Tilbrook, B. (2018). Distribution of planktonic biogenic carbonate organisms in the Southern Ocean south of Australia: A baseline for ocean acidification impact assessment. *Biogeosciences*, 15(1), 31–49. <https://doi.org/10.5194/bg-15-31-2018>
- Yoder, J. A., McClain, C. R., Feldman, G. C., & Esaias, W. E. (1993). Annual cycles of phytoplankton chlorophyll concentrations in the global ocean: A satellite view. *Global Biogeochemical Cycles*, 7(1), 181–193. <https://doi.org/10.1029/93GB02358>